phys. stat. sol. (c) **0**, No. 7, 2339–2342 (2003) / **DOI** 10.1002/pssc.200303545

Magnetotransport measurement of effective mass, quantum scattering time, and alloy scattering potential of polarization-doped 3D electron slabs in graded-AlGaN

Debdeep Jena[*, 1], **S. Heikman**[1], **J. S. Speck**[1], **U. K. Mishra**[1], **A. Link**[2], and **O. Ambacher**[2]

[1] Department of Electrical and Computer Engineering and Materials Department, University of California, Santa Barbara, USA
[2] Walter Schottky Institut, Am Coulombwall, 85748 Garching, Germany

Received 9 April 2003, accepted 10 September 2003
Published online 12 November 2003

PACS 73.50.Jt, 73.63.–b

By applying the technique of polarization bulk-doping in graded AlGaN, it has been possible to create high-mobility three-dimensional electron slabs. Such 3D electron slabs are observed to exhibit clearly resolved Shubnikov de-Haas oscillations. From a temperature-dependent study of the oscillations, we measure the effective mass ($m^* = 0.21 m_0$) and the quantum scattering time ($\tau_q = 0.3$ ps) of carriers in the slabs. An analysis of the ratio of quantum and classical scattering times with the scattering mechanisms leads to the *first direct measurement* of the alloy scattering potential in the AlGaN system ($V_0 = 1.8$ eV).

1 Introduction We recently demonstrated [1] the realization of polarization-doped 3D electron slabs (3DES) in graded AlGaN/GaN heterostructures. This is depicted schematically in Fig. 1a. Grading of $Al_xGa_{1-x}N$ grown epitaxially on GaN causes a non-vanishing polarization in the growth direction, which causes a fixed polarization charge ($N_\pi^D = \nabla \cdot \boldsymbol{P}$). The fixed charge distribution attracts free carriers resulting in the formation of a mobile 3DES. Such 3DES carriers do not freeze out at low temperatures as opposed to traditional shallow donor-doped carriers. There is a large improvement in the low temperature mobility due to the reduction of ionized impurity scattering, resulting in high mobilities of $\mu \approx 3000$ cm^2/V s at a carrier density $n_{3d} = 10^{18}$ cm^{-3} for $T \leq 20$ K. As shown in [1] by capacitance-voltage profiling, the carriers are observed to be indeed three-dimensional, caused by the fixed polarization background charge.

We have observed clearly resolved Shubnikov de-Haas oscillations in such polarization-doped 3DES. Analysis of the temperature-dependent oscillations enables us to measure the electron effective-mass, the quantum scattering time, and most importantly, the alloy scattering potential in AlGaN.

2 Experiment The sample (Fig. 1a) is a Ga-face structure grown along the polar c(0001) axis by plasma-induced MBE [2] on a MOCVD-grown semi-insulating [3] GaN on a sapphire substrate. The top 100 nm of the structure is linearly graded AlGaN; the composition of Al is changed from 0–30% by controlling the aluminum flux by a computer program [1]. The 3DES formed by polar-

[*] Corresponding author: e-mail: djena@nd.edu, Phone: +01 574 631 8835, Fax: +01 574 631 4393

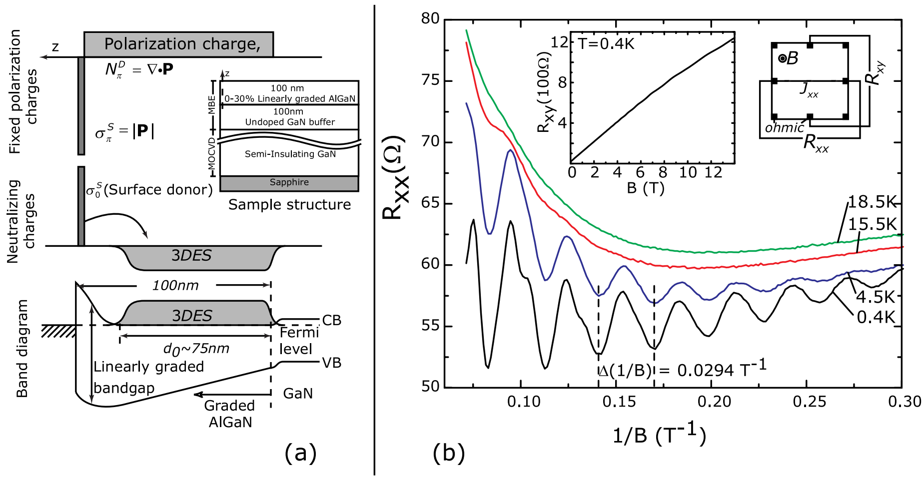

Fig. 1 (online colour at: www.interscience.wiley.com) Part (a) shows the fixed polarization charge, the mobile 3DES, and the schematic band-diagram with the sample structure used for the experiment. Part (b) shows the measured Shubnikov de-Haas oscillations in R_{xx} against $1/B$ with insets of the Van-der Pauw geometry used and the $R_{xy} - B$ plot for 0.4 K. The oscillations are periodic with a period $\Delta(1/B) = 0.0294\ \mathrm{T}^{-1}$.

ization doping has a temperature-independent electron *sheet*-density $n_{2d} = 7.5 \times 10^{12}\ \mathrm{cm}^{-2}$ and a mobility $\mu = 2700\ \mathrm{cm}^2/\mathrm{V\,s}$ at $T = 20$ K, measured by conventional low-B field Hall measurement.

For magnetotransport measurements of the 3DES, ohmic contacts were formed in a Van-der Pauw geometry (Fig. 1b inset). The sample was immersed in a ^{3}He low-temperature cryostat with a base temperature of 300 mK. Magnetic fields in the range $0\ \mathrm{T} \le B \le 14\ \mathrm{T}$ were applied. R_{xx} and R_{xy} was measured as in the geometry depicted in the figure using the standard low-frequency lock-in technique. Magnetotransport measurements were carried out by Link et al. at WSI, Munich.

Figure 1b shows the measured R_{xx} against $1/B$ for four temperatures. The inset is the geometry of contacts and a plot of measured R_{xy} against B for $T = 0.4$ K. The Hall mobility determined from the slope of the R_{xy} curve is $\mu_H \simeq 3000\ \mathrm{cm}^2/\mathrm{V\,s}$, and the Hall 3-D carrier density is $n_{3d} \sim 10^{18}/\mathrm{cm}^3$.

The oscillatory component of the transverse magnetoresistance component ΔR_{xx} is given by [4]

$$\Delta R_{xx}^{\mathrm{osc}} = \frac{\chi}{\sinh \chi}\, \mathrm{e}^{-\pi/\omega_c \tau_q} \left(\frac{\hbar \omega_c}{2\varepsilon_F}\right)^{1/2} \cos\left(\frac{2\pi \varepsilon_F}{\hbar \omega_C}\right), \qquad (1)$$

where $\chi = 2\pi^2 k_B T/\hbar\omega_c$, $\omega_c = eB/m^*$ is the cyclotron frequency, τ_q is the quantum scattering time, and $\varepsilon_F = \hbar^2 k_F^2/2m^*$ is the Fermi-energy with $k_F = (3\pi^2 n_{3d})^{1/3}$. This is periodic in $1/B$, as is seen in Fig. 1b.

The R_{xx} oscillation period $\Delta(1/B) = 2e/\hbar(3\pi^2 n_{3d})^{-2/3} = 0.0294\ \mathrm{T}^{-1}$ (Fig. 1b) gives a 3-D carrier concentration $n_{3d} = 1.1 \times 10^{18}\ \mathrm{cm}^{-3}$, which is in close agreement with the carrier density inferred from the classical Hall and C-V measurements. For finding the effective mass and quantum scattering time, a FFT-filter is used to remove the background resistance in Fig. 1b, and only the oscillatory part is retained.

2.1 Effective mass The effective mass of carriers is determined by fitting [5] the measured amplitude damping of ΔR_{xx} with temperature at fixed B to the temperature-damping term of Eq. (1), $\chi/\sinh\chi$. From the fit (shown in Fig. 2a), the effective mass is found to be $m^* = 0.21 m_0$. The band-edge electron effective mass in pure GaN (AlN) is $m^*_{\mathrm{GaN}} = 0.20 m_0$ ($m^*_{\mathrm{AlN}} = 0.32 m_0$) [6]. From a linear interpolation for the 3DES experiencing an average Al-composition of $\langle x \rangle = 0.11$ we expect an effective mass of $0.21 m_0$, which is in good agreement with the measured value.

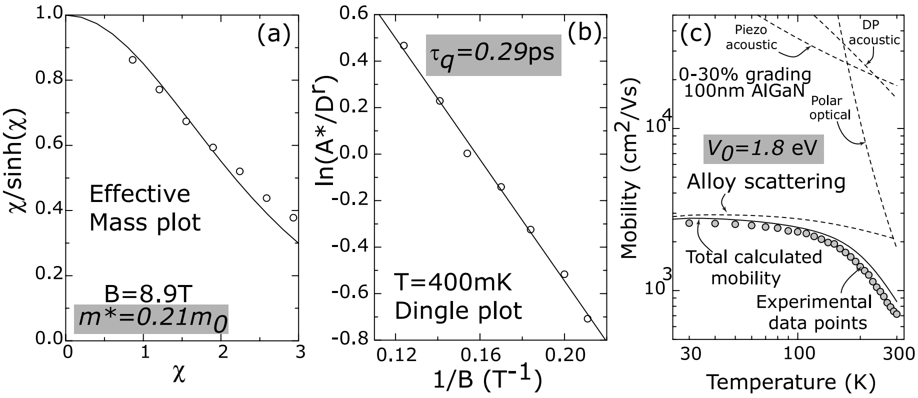

Fig. 2 Part (a) is the effective mass plot yielding the effective mass of $m^* = 0.21 m_0$. Part (b) is the Dingle plot yielding a quantum scattering time of $\tau_q = 0.3$ ps. Part (c) shows the measured and calculated mobility as a function of temperature. The effect of alloy scattering is seen to be rather strong for the entire temperature range; the reduction in mobility at high temperatures results from optical phonon scattering combined with alloy scattering. Other scattering mechanisms do not contribute strongly to the mobility.

2.2 Scattering time–quantum and classical From Eq. (1), the slope of the Dingle plot [7] (Fig. 2b), i.e., $\ln [A^*/(\sqrt{\hbar\omega_c/2\varepsilon_F}\chi/\sinh \chi)]$ (A^* stands for peak values of the oscillation) plotted against $1/B$ yields a quantum scattering time of $\tau_q = 0.29$ ps. An averaging of the quantum scattering times over a range of low temperatures yields a value $\tau_q^{\mathrm{av}} = 0.3$ ps.

2.3 Alloy scattering potential Alloy scattering is identified as the dominant scattering mechanism at low temperatures, and is rather strong even at high temperatures. Alloy scattering potential V_0 is of a short range nature, which makes the scattering process isotropic and the ratio of classical [8] and quantum scattering times $\tau_c/\tau_q \sim 1$, as observed. The scattering rate due to alloy disorder with a short range potential V_0 for a degenerate 3DES is given by [9]

$$\frac{1}{\tau_{\mathrm{alloy}}} = \frac{2\pi}{\hbar} V_0^2 \Omega(x)\, x(1-x)\, g_{3D}(\varepsilon_F)\,, \tag{2}$$

where $\Omega_0(x)$ is alloy composition-dependent volume of the unit cell over which the alloy scattering potential V_0 is effective, and x is the alloy composition. $g_{3D}(\varepsilon)$ is the 3-dimensional density of states. Since the alloy is graded Matheissen's rule is used for a spatial averaging of the scattering rate

$$\langle \tau_{\mathrm{alloy}}^{-1} \rangle = \frac{1}{x_0} \int_0^{x_0} \tau_{\mathrm{alloy}}^{-1}(x)\, \mathrm{d}x\,, \tag{3}$$

where $x_0 = 0.225$ is the alloy composition experienced by 3DES electrons at the top edge of the depletion region. Using this simple result we calculate mobility as a function of temperature for the 3DES. This is shown along with the measured temperature-dependent mobility in Fig. 2c. We conclude that to achieve a low-temperature transport mobility of $3000\,\mathrm{cm^2/V\,s}$, an alloy scattering potential of $V_0 = 1.8$ eV is necessary. Due to the lack of experimental values, it has been common practice to assume the scattering potential to be the conduction band offset between the binaries forming the alloy ($V_0 = \Delta E_c = 2.1$ eV for AlN, GaN) [6]. With an alloy scattering potential of $V_0 = 2.1$ eV, the calculated mobility is *much lower* ($\approx 2000\,\mathrm{cm^2/V\,s}$) than the measured value. The 3DES mobility is dominated by alloy scattering and all other scattering mechanisms are removed, making it a clean measurement of the alloy scattering potential. This report presents the *first measurement* of the alloy scattering potential in AlGaN material system.

3 Conclusions In summary, we observe Shubnikov de-Haas oscillations of a degenerate 3DES realized by the novel technique of polarization bulk-doping in graded AlGaN layers. The effective mass of electrons in the graded AlGaN layer was measured from temperature dependence of oscillations to be ($m^* = 0.21 m_0$) and their quantum scattering time was measured to be ($\tau_q = 0.3$ ps). Alloy scattering was identified as the dominant scattering mechanism (and confirmed from the measured ratio of classical and quantum scattering times), making it possible to measure the alloy scattering potential ($V_0 = 1.8$ eV).

Degenerate three-dimensional electron gases have many applications such as the study of collective phenomena (spin-density waves, Wigner crystallization, and integral and fractional quantum-Hall effects in 3-dimensions [10]). Polarization-doped electron slabs provide a novel technique of creating such electron populations, overcoming the thermal freezeout effects associated with *impurity-doped* semiconductors. The wide *tunability* of slab thickness and electron density offered by polarization-doping makes it an attractive system for the study of dimensionality and confinement on carrier transport.

Acknowledgements Funding from POLARIS/MURI (Contract monitor: C. Wood) is gratefully acknowledged.

References

[1] D. Jena, S. Heikman, D. Green, D. Buttari, R. Coffie, H. Xing, S. Keller, S. P. DenBaars, J. S. Speck, U. K. Mishra, and I. P. Smorchkova, Appl. Phys. Lett. **81**, 4395 (2002).
[2] B. Heying, R. Averbeck, L. F. Chen, E. Haus, H. Reichert, and J. S. Speck, J. Appl. Phys. **88**, 1855 (2000).
[3] S. Heikman, S. Keller, S. P. DenBaars, and U. K. Mishra, Appl. Phys. Lett. **81**, 439 (2002).
[4] R. Kubo, H. Hasegawa, and N. Hashitume, J. Phys. Soc. Jpn. **14**, 56 (1959).
[5] R. J. Sladek, Phys. Rev. **110**, 817 (1958).
[6] I. Vurgaftman, J. R. Meyer, and L. R. Ram-Mohan, J. Appl. Phys. **89**, 9815 (2001).
[7] R. B. Dingle, Proc. R. Soc. Lond. A **211**, 517 (1952).
[8] Classical scattering time τ_c is related to the measured mobility by the Drude relation $\mu = e\tau_c/m^*$.
[9] C. Hamaguchi, Basic Semiconductor Physics (Springer-Verlag, Berlin, 2001).
[10] A. C. Gossard, M. Sundaram, and P. F. Hopkins, in: Epitaxial Microstructures, edited by A. C. Gossard, Semiconductors and Semimetals **40** (Academic Press, San Diego, 1994).